Surface investigation and aluminum oxide estimation on test filters for the ATHENA X-IFU and WFI detectors

Luisa Sciortino*[1], Ugo Lo Cicero[2], Elena Magnano [3,4], Igor Píš [5], and Marco Barbera [1,2].
[1]Università degli Studi di Palermo, Dipartimento di Fisica e Chimica, Via Archirafi 36, 90123 Palermo, Italy; [2]Istituto Nazionale di Astrofisica, Osservatorio Astronomico di Palermo, Piazza del Parlamento 1, 90134 Palermo, Italy; [3]Consiglio Nazionale delle Ricerche, Istituto Officina dei Materiali, Laboratorio TASC, Strada Statale 14, Km.163.5 in Area Science Park, 34149 Basovizza, Trieste, Italy; [4]Department of Physics, University of Johannesburg, PO Box 524, Auckland Park 2006, South Africa; [5]Elettra-Sincrotrone Trieste S.C.p.A., Strada Statale 14, Km.163.5 in Area Science Park, 34149 Basovizza, Trieste, Italy
Corresponding Author: luisa.sciortino@unipa.it

ABSTRACT

The ATHENA mission provides the demanded capabilities to address the ESA science theme "Hot and Energetic Universe". Two complementary instruments are foreseen: the X-IFU (X-ray Integral Field Unit) and WFI (Wide Field Imager). Both the instruments require filters to avoid that the IR radiation heats the X-IFU cryogenic detector and to protect the WFI detector from UV photons. Previous experience on XMM filters recommends to employ bilayer membrane consisting of aluminum deposited on polyimide. In this work, we use the X-ray Photoelectron Spectroscopy (XPS) to quantify the native aluminum oxide thickness that affects the spectral properties of the filter. The estimation of the oxide thickness of the prototype filter for ATHENA is a considerable information for the conceptual design of the filters.

Keywords: Athena mission, thermal filters, aluminum oxide.

Space Telescopes and Instrumentation 2016: Ultraviolet to Gamma Ray, edited by
Jan-Willem A. den Herder, Tadayuki Takahashi, Marshall Bautz, Proc. of SPIE Vol. 9905, 990566
 · doi: 10.1117/12.2232376

1. INTRODUCTION

ATHENA is a large astrophysics space mission[1] recently selected by the European Space Agency (launch scheduled in 2028) to address the science theme "Hot and Energetic Universe". It will be equipped with two interchangeable focal plane instruments that are designed with different characteristics. One of the two instruments on-board ATHENA is the X-ray Integral Field Unit (X-IFU)[2] an x-ray detector with spectral, imaging and timing capabilities in the energy range 0.2÷12 keV based on an array of Transition Edge Sensor (TES) micro-calorimeters. The X-IFU, operating at temperatures below 100 mK [3] will be mounted inside a sophisticated cryostat [4] at the focal plane of a large area and high angular resolution grazing incidence X-ray telescope. In order to allow the focused X-ray beam to reach the X-IFU detector a clear path (aperture cylinder) has to be opened in the cryostat thermal and mechanical shields.[5] Such openings need to be shielded by thin thermal filters, that block IR radiation while being nearly transparent to X-rays in the energy band 0.1-12 keV, to avoid additional thermal load on the low temperature detectors and to prevent energy resolution degradation due to photon shot noise.[6]

The Wide Field Imager (WFI), the other instrument for the ATHENA mission, conjugated a large field of view of 40 arcmin with a high count rate capability.[7] This required performance is achieved by the use of DEPFET active pixel sensor matrices. DEPFETs, however, are also sensitive to UV photons, and thus a large area X-ray transparent optical blocking filter, mounted on a filter wheel, will be used to attenuate optical radiation when observing bright UV/Vis sources, to avoid spectral resolution degradations and energy scale variations.[8]

In the current baseline design both the X-IFU thermal filters and WFI optical blocking filters are made of two stacked thin layers of aluminum and polyimide. Both materials are characterized by high transmission in X-rays, while the metallic aluminum blocks the Vis/IR components mainly by reflection and the polyimide blocks the UV component by absorption.[9] These blocking properties could be exploited for the X-IFU and WFI design, respectively.

The thickness of the aluminum layer should be kept to the minimum value providing adequate reflectivity in the Vis/IR and UV absorption, to maximize the X-ray transmissivity, in particular below 1 keV where key spectral features are expected for many astrophysical sources in the ATHENA science program.[1] However, aluminum in air always forms a nanometric film of native oxide that presents very different spectral properties. In contrast with the metallic aluminum, the oxide is less efficient to reflect IR radiation and is nearly transparent to UV/Vis radiation. Since the mass ratio between aluminum oxide and metallic aluminum increases in nanomaterials, the changes in the spectral properties are more dramatic for nanometric films.

In this work we employ synchrotron-excited X-ray Photoelectron Spectroscopy (XPS) with different incident energies to probe the surface (few nanometers) of a prototype filter consisting of aluminum deposited on polyimide. We analyze XPS spectra to estimate the thickness of the native oxide that alters unfavorably the transmission of the filters. Such knowledge is a critical information to design appropriately the flight filters.

2. MATERIALS AND METHODS

We purchased a prototype filter by LUXEL Corporation, here named S150 (TF111-2677 R/N 34498-2), consisting of aluminum (purity 99.999%) with nominal thickness 28.8 nm deposited on polyimide with nominal thickness of 153.4 nm. This bilayer membrane is mounted on an anodized aluminum frame by the company.
During the measurements the sample was electrically linked to the ground through a silver wire to avoid charge accumulation on the surface (figure 1).

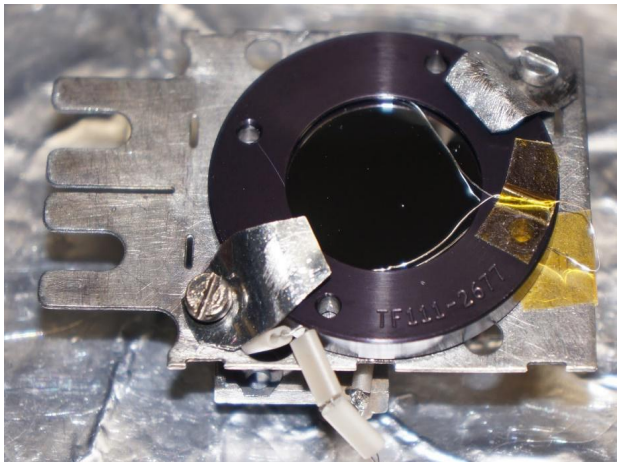

Figure 1. S150 filter grounded with a silver wire.

We performed X-ray Photoelectron Spectroscopy (XPS) at the BACH beamline of the Italian synchrotron ELETTRA (proposal number 20150287) probing the metallic surface (few nanometers) of the filter. The measurements were carried out at room temperature with four different incident energies 609, 806, 1040, and 1497 eV, the total energy resolution was set to 0.3, 0.3, 0.4, and 0.6 eV, respectively. The experimental geometry is sketched in figure 2. The angle θ, between the XPS detector and the surface of the sample was set to 90° for all measurements, while the angle between incident beam and the detector is fixed at 60° in the beamline setup.

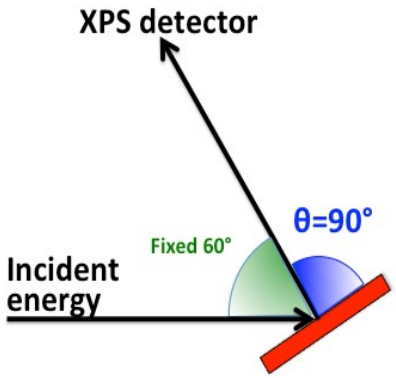

Figure 2. Geometrical setup for the XPS measurement performed at BACH beamline.

The photoelectron binding energies were calibrated by measuring Au 4f spectrum of a gold reference sample. The investigated spectral region is the Al 2p core level.

3. RESULTS AND DISCUSSION

3.1 Data analysis

XPS was used to study the metallic surface of the filters, all experimental scans of the Al 2p peaks are reported after area normalization in figure 3. Two well-distinguished signals of aluminum are recognizable close to 73.0 and 75.6 eV binding energy (BE), respectively, as it is evident in figure 3. Generally, peaks at higher binding energy are originated from elements in higher oxidation states. The peak at higher binding energy is ascribed to the Al^{3+} component, while the signal at lower binding energy is attributed to the Al^{0} component.[10] As expected for a surface oxidation the area of the

peak ascribed to the oxide increases when the incident energy decreases as a result of the lower attenuation length of the electrons in the material.

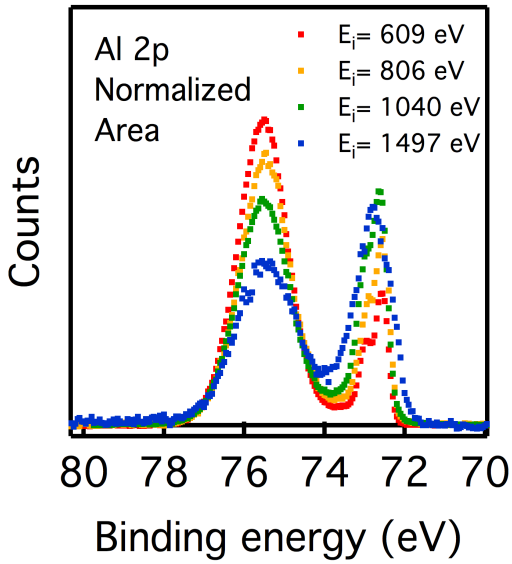

Figure 3. Al 2p XPS spectra of the sample S150 at different incident energies: 609 eV (red), 806 eV (orange), 1040 eV (green), and 1497 eV (blue). Spectra are normalized by the total spectrum area after the background subtraction.

In all analysis a Shirley background has been subtracted to the raw data and for the fits of the Al 2p peak three spectral components have been taken into account one for the oxide and two for the metal, these last two are a doublet due to the spin-orbit coupling. Indeed, by inspection of figure 3, it is possible to recognize two maxima for the Al^0 and only one for the Al^{3+} component. The Al^0 signal is typified by a doublet corresponding to the two possible states having different binding energies, then we can observe the two peaks, $2p_{1/2}$ and $2p_{3/2}$. Although the energy separation between the two maxima of the doublet is often not resolved using laboratory sources, in our data the splitting is easily recognizable because of the high energy resolution of the data that allows to distinguish the $2p_{1/2}$ and $2p_{3/2}$ components.

Fits have been carried out using the XPST program package,[11] each peak is reproduced by Gauss-Lorentzian (70%-30%) sum function to approximate the Voigt profile. The Full Width at Half Maximum for the Al^0 $2p_{1/2}$ and to the Al^0 $2p_{3/2}$ signals is constrained to be identical and the ratio of area is constrained to be 1:2 as expected from theory.

Example of the Al 2p spectrum decomposed into the three above mention components is given in Figure 4 for the photon energy of 609 eV.

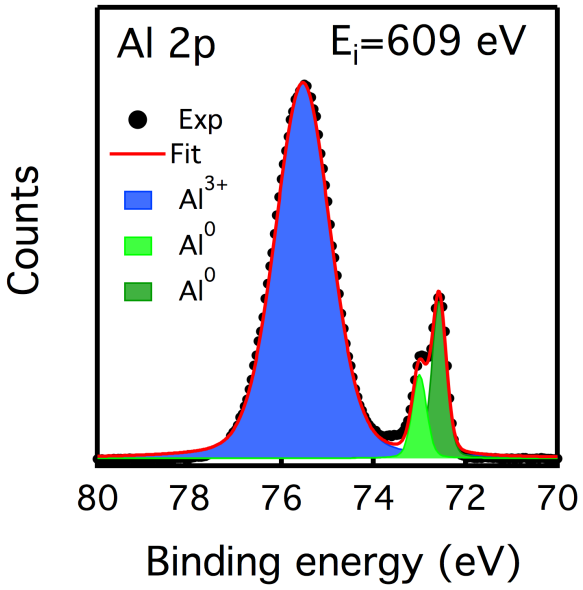

Figure 4. XPS scan for the Al 2p binding energy with incident energy 609 eV of the sample S150. Data reported are experimental (black full circle), best fit (red line), Al3+ 2p component (blue filled curve) Al0 2p1/2 (light green filled curve), and Al0 2p3/2 (dark green filled curve).

3.2 Superficial aluminum oxide estimation

Assuming a flat homogenous oxide layer on top of a homogenous Al substrate, the thickness of aluminum oxide can be calculated using equation 1 [12]:

$$d = \lambda_o \sin\theta \ln\left(\frac{N_m \lambda_m}{N_o \lambda_o}\frac{I_o}{I_m} + 1\right) \qquad (1)$$

where d is the thickness of the oxide layer, λ_o and λ_m are the electron inelastic mean free paths (IMFP) in the oxide and the metal, respectively, θ is the electron take-off angle with respect to surface sample, N_o and N_m are the volume densities of the aluminum atoms in the oxide and the metal, respectively, and the I_o and I_m are the peak areas of the oxide and metal component of the Al 2p signal. The volume densities of the aluminum atoms in aluminum oxide is correlated to the presence of other elements with a typical Nm/No ratio in the range 1.3-1.5, albeit in this paper to estimate the oxide thickness by eq.1 a Nm/No ratio of 1.5 is used as was done previously.[13] To account for the effects of elastic-electron scattering, electron effective attenuation length (EAL) instead of IMFP can be used.[14] The EALs were calculated using the NIST EAL database [15] and the values corresponding to the used incident photon energies are listed in Table 1.

Table 1. Calculated average practical EAL[§] in Al and Al_2O_3 for photoelectrons excited from the Al 2p core level.

Photon energy (eV)	EAL in Al (nm)	EAL in Al_2O_3 (nm)	I_m %	I_o %
609	1.1±0.1	1.3±0.2	14	86
806	1.4±0.2	1.7±0.3	23	77
1040	1.8±0.2	2.2±0.4	31	69
1497	2.4±0.3	3.0±0.5	42	58

[§]The EALs are calculated using the NIST EAL database [15] and the TPP-2M predictive formula [16] assuming the density of 3.3 g cm^{-3}, band gap energy 7.0 eV [17] and 24 valence electrons per molecule for the Al_2O_3 over-layer.[15] The values of the photoionization asymmetry parameter were taken from ref.[18] The uncertainty of 10.9 and 17.4 % is considered for Al and Al_2O_3, respectively [15] I_o and I_m are the peak areas of the oxide and metal component of the Al 2p signal.

The plot of λ_o vs the inverse of the logarithm of eq.1 is reported in figure 5. Then according to eq.1 the oxide thickness is calculated as the slope of the linear fit, that gives the thickness of Al_2O_3 equal to 2.85±0.25 nm.

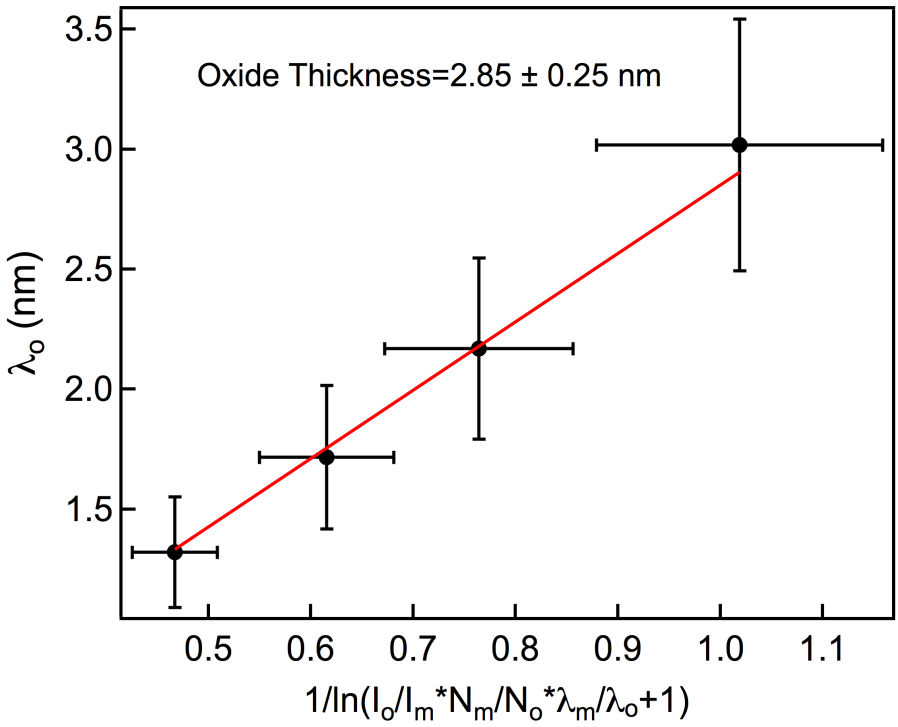

Figure 5. Plot of λ_o vs the inverse of the logarithm of eq.1 (black circles) and linear fit (red line).

Such value is in good agreement with the thickness of native oxide on bulk Al(111) and Al(100) crystals [10] but it is very different to the case of the XMM thin and medium filters [19] where the aluminum oxide thickness was found to be 5.9 nm, thus nearly twice that measured in this work for the LUXEL filter sample. Since native oxide is stable after its formation and since the investigated prototype filter shows lower amount of aluminum oxide with respect to the XMM filters, we can design the ATHENA filters with a lower thickness of aluminum thus improving the low energy X-ray transmission. The lower amount of aluminum oxide in the investigated sample is likely due to the deposition process specifically developed by LUXEL for Polyimide substrates which likely produces more compact aluminum layers (LUXEL private communication).

4. SUMMARY AND CONCLUSIONS

As part of the ATHENA phase-A study activities we are investigating the performances of filter materials suitable for the design of the X-IFU thermal filters and WFI optical blocking filter. Here we report the results of X-ray Photoelectron Spectroscopy measurements performed at ELETTRA synchrotron in Trieste to measure the thickness of the surface aluminum oxide. This measurement is relevant since the aluminum oxide reduces the efficiency of bulk aluminum in reflecting IR and absorbing UV/VIS light.

The analysis of the XPS spectra provides a value of < 3 nm for the thickness of the surface aluminum oxide measured on filter samples manufactured by LUXEL. Such result is very different from what we measured in the past on XMM thin and medium filters manufactured by MOXTEK [19] where the aluminum oxide thickness was nearly twice that measured in this work.

Based on such encouraging results we think that, in principle, it is possible to reduce the total amount of aluminum in order to maximize the X-ray transmissivity. We plan to perform Atomic Force Microscopy investigation on the LUXEL aluminum/polyimide samples to measure the surface micro-roughness and compare it with what we have already measured on XMM filter samples.

ACKNOWLEDGEMENTS

The research leading to these results has received funding from ASI (Italian Space Agency) through the Contract n. 2015-046-R.0 and from the European Union's Horizon 2020 Programme under the AHEAD (Integrated Activities in the High Energy Astrophysics Domain) project (grant agreement n. 654215).

REFERENCES

[1] Barcons, X., Nandra, K., Barret, D., den Herder, J.-W., Fabian, A. C., Piro, L., Watson, M. G., and the Athena team, "Athena: the X-ray observatory to study the hot and energetic Universe", Journal of Physics Conference Series, 610 (1) 012008 (2015)

[2] Ravera L., Barret D., den Herder J.W., Piro L., Cledassou R., Pointecouteau E., Philippe Peille, Pajot F., Arnaud M., Pigot C., Duband L., Cara C., den Hartog R.H., Gottardi L., Akamatsu H., van der Kuur J., van Weersc H.J., de Plaac J., Macculi C., Lotti S., Torrioli G., Gatti F., Valenziano L., Barbera M., Barcons X., Ceballos M.T., Fabrega L., Mas-Hesse J.M., Page M.J., Guttridge P.R., Willingale R., Fraser G.W., Paltani S., Genolet L., Bozzo E., Rauw G., Renotte E., Wilms J., and Schmidt C., "The X-ray integral field unit (X-IFU) for Athena", Proc. SPIE, 9144 (2014)

[3] Branco M. B. C., Charles I., Butterworth J., "ATHENA X-IFU detector cooling chain", Proc. SPIE, 9144 (2014)

[4] Duband L., Charles I., Duval J.M., "Coolers development for the ATHENA X-IFU cryogenic chain", Proc. SPIE 9144 (2014)

[5] Barbera M., Argan A., Bozzo E., Branduardi-Raymont G., Ciaravella A., Collura A., Cuttaia F., Gatti F., Jimenez Escobar A., Lo Cicero U., Lotti S., Macculi C., Mineo T., Nuzzo F., Paltani S., Parodi G., Piro L., Rauw G., Sciortino L., Sciortino S., Villa F., "Thermal Filters for the ATHENA X-IFU: Ongoing Activities Toward the Conceptual Design", Journal of Low Temperature Physics, 1-6 (2016)

[6] Barbera M., Collura A., Gatti F., Lo Cicero U., Macculi C., Piro L., Renotte E., Sciortino S., "Baseline design of the thermal blocking filters for the X-IFU detector on board ATHENA", Proc. SPIE, 9144 (2014)

[7] Meidinger N., Nandra K., Plattner M., Porro M., Rau A., Santangelo A., Tenzer C., and Wilms J., "The wide field imager instrument for Athena", Proc. of SPIE, 9144 (2014)

[8] a) Barbera M., Branduardi-Raymont G., Collura A., Comastri A., Eder J., Kamisiński T., Lo Cicero U., Meidinger N., Mineo T., Molendi S., Parodi G., Pilch A., Piro L., Rataj M., Rauw G., Sciortino L., Sciortino S., Wawer P., "The optical blocking filter for the ATHENA wide field imager: ongoing activities towards the conceptual design" Proc. SPIE, 9601 (2015); b) Rataj M., Polak S., Palgan T., Kasimiński T., Pilch A., Eder J., Meidinger N., Plattner M., Barbera M., D'Anca F., Parodi G., "The Filter and Calibration Wheel for the ATHENA Wide Field Imager " Proc. SPIE, 9905, this conference.

[9] Barbera M., Austin K., Collura A., Flanagan A., Jelinsky R., Murray S., Serio S., Zombeck M., "Development of the UV/ion shields for the Advanced X-ray Astrophysics Facility high-resolution camera (AXAF HRC)", Proc. SPIE, 2280 (1994)

[10] Evertsson J., Bertram F., Zhang F., Rullik L., Merte L.R., Shipilin M., Soldemo M., Ahmadi S., Vinogradov N., Carlà F., Weissenrieder J., Göthelid M., Pan J., Mikkelsen A., Nilsson J.O., Lundgren E., "The thickness of native oxides on aluminum alloys and single crystals", Applied Surface Science, 349, 826–832 (2015)

[11] Schmid M., Steinrück H.P. and Gottfried J.M. “A new asymmetric Pseudo-Voigt function for more efficient fitting of XPS lines” Surf. Interface Anal. (2014)
[12] Carlson, T. A. “Basic assumptions and recent developments in quantitative XPS” Surf. Interface Anal., 4, 125–134 (1982)
[13] Strohmeier, B. R. “An ESCA method for determining the oxide thickness on aluminum alloys”, Surface and Interface Analysis, 15(1), 51-56 (1990).
[14] Jablonski A., Powell C.J., “The electron attenuation length revisited”, Surface Science Reports, 47, 33-91 (2002)
[15] Powell C. J. and Jablonski A., NIST Electron Effective-Attenuation-Length Database - Version 1.3, National Institute of Standards and Technology, Gaithersburg, MD (2011)
[16] Tanuma, S., Powell, C. J., and Penn, D. R., “Calculations of electron inelastic mean free paths” Surf. Interface Anal. 21, 165 (1994)
[17] Filatova E.O. and Konashuk A.S., “Interpretation of the Changing the Band Gap of Al_2O_3 Depending on Its Crystalline Form: Connection with Different Local Symmetries”, J. Phys. Chem. C, 119(35), 20755–20761 (2015)
[18] Yeh J.J. and Lindau I., “Atomic subshell photoionization cross sections and asymmetry parameters: 1□Z□103”, Atomic Data and Nuclear Data Tables, 32, 1-155 (1985)
[19] Barbera M., Agnello S., Buscarino G., Collura A., Gastaldello F., La Palombara N., Lo Cicero U., Tiengo A., Sciortino L., Varisco S., Venezia A.M., “Status of the EPIC thin and medium filters on-board XMM-Newton after more than 10 years of operation: 1) laboratory measurements on back-up filters”, Proc. of SPIE, 8859 (2013)